Supporting Material for

Bicelles and Other Membrane Mimics: Comparison of Structure, Properties, and Dynamics from MD Simulations

Mikkel Vestergaard[#], Johan F. Kraft[#], Thomas Vosegaard[€], Lea Thøgersen[‡,†], and Birgit Schiøtt[#]*

[#]Center for Insoluble Protein Structures (inSPIN), Interdisciplinary Nanoscience Center (iNANO), and Department of Chemistry, Aarhus University, Langelandsgade 140, DK-8000 Aarhus C, Denmark

[€]Danish Center for Ultrahigh-Field NMR Spectroscopy and Center for Insoluble Protein Structures (inSPIN), Interdisciplinary Nanoscience Center (iNANO) and Department of Chemistry, Aarhus University, Gustav Wieds Vej 14, DK-8000 Aarhus C, Denmark

[‡]Center for Membrane Pumps in Cells and Disease (PUMPKIN), Bioinformatics Research Centre, Aarhus University, C.F. Møllers Alle 8, DK-8000 Aarhus C, Denmark

[†]Current address: QIAGEN-Aarhus, Silkeborgvej 2, DK-8000 Aarhus C, Denmark

*To whom correspondence should be addressed: Birgit Schiøtt; E-mail: birgit@chem.au.dk; Phone: +45 8715 5975; Fax: +45 8619 6199

Simulation Setups

Membrane Mimics. A bilayer with a size of 10.7 nm x 10.7 nm consisting of 300 lipids was constructed with the membrane builder plugin for VMD[1], converted to a CG description, and solvated with 6114 water beads to a total box size of 10.7 nm x 10.7 nm x 10.7 nm. This system was simulated for 2000 ns (simulation named *Bilayer*). For construction of some of the other membrane mimics (see below) a 100 nm x 100 nm bilayer was formed by replicating the initial bilayer 10 times in both dimensions of the bilayer plane and equilibrating it for 1 ns.

The q=0.5 bicelles were modelled in two ways; either they were created from self-assembly of a random distribution of lipids or they were cut as a disc with a radius of 3 nm or 5 nm from the large equilibrated DMPC bilayer described above followed by randomly selecting lipids for mutation to DHPC to achieve the desired q-value. Afterwards, all q=0.5 bicelle systems were equilibrated by use of a simulated annealing (SA) protocol for obtaining equilibrated bicelles. This was necessary due to the very large uncertainty in the real size of these structures[2-4] and the slow equilibration of this type of systems (see Figure S1). To find the most efficient way of reaching equilibrium, different simulated annealing protocols were tested by varying the annealing temperature, T_{max}, and the length of the time intervals t_{init}, t_{heat}, t_{max} and $t_{cooldown}$ (see Figure S2).

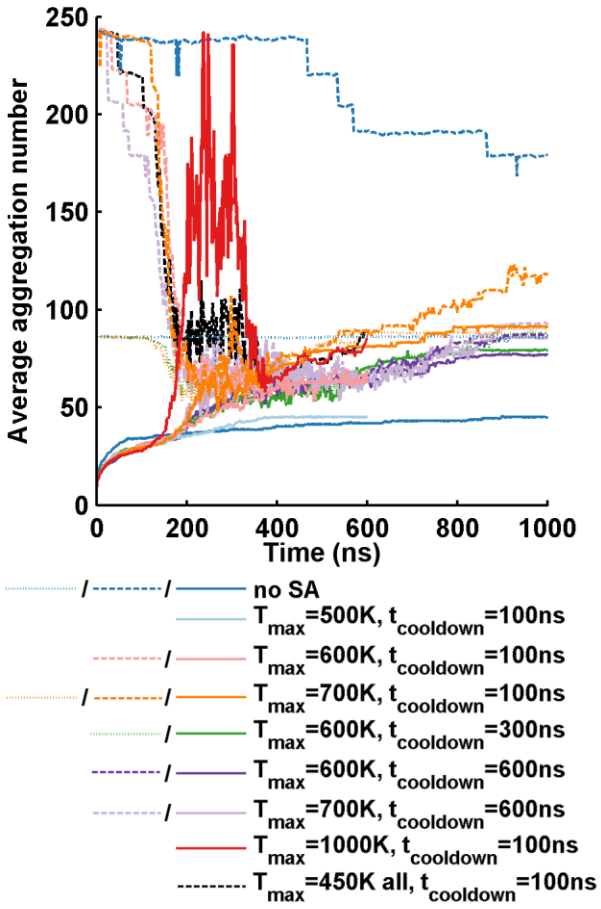

Figure S1. The average aggregation number as function of time. The simulations are started from a random distribution of lipids (full lines), discs with a radius of 3 nm (dotted lines), and discs with a radius of 5 nm (broken lines).

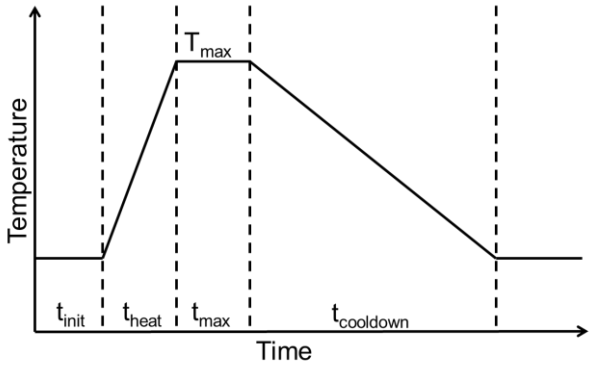

Figure S2. Schematic representation of the simulated annealing protocol.

Initially, t_{init}, t_{heat}, t_{max} and $t_{cooldown}$ were all set to 100 ns, while the annealing temperature T_{max} was varied and simulations starting from different starting conditions were compared. The average aggregation number over time is plotted in Figure S1. Three different starting conditions were tested: Lipids randomly distributed in a box (full lines), discs with a radius of 3 nm (dotted lines), and discs with a radius of 5 nm (broken lines). When the temperature was increased after 100 ns, the bicelles started from a 5 nm disc started to fall apart and the average aggregation number decreased. In the simulations started from a random composition of lipids, the lipids started to form larger structures and the average aggregation number increased. After 200 ns the temperature was kept fixed at T_{max} for 100 ns and the change in average aggregation number continued. During the cooldown period from 300 to 400 ns the aggregation number increased further. This was because the free DHPC concentration doing the increased temperature period was larger than at room temperature (see Figure S3) and doing the cooling the free DHPC started to adhere to the other aggregates. In the following equilibration period the aggregation number continued to increase a bit, however, a final plateau was about to be reached. It was found that heating the lipids alone with an annealing temperature of 700 K and above gave similar average aggregation numbers independent of the temperature. It was furthermore found that this temperature was high enough to obtain the same average aggregation number when starting from the three different starting configurations. Therefore, 700K was chosen as the annealing temperature. The size of these bicelles fitted the smallest values previously found.[2,5] No consistent bicelle size matching the larger experimental values[3] was obtained with any of the annealing protocols.

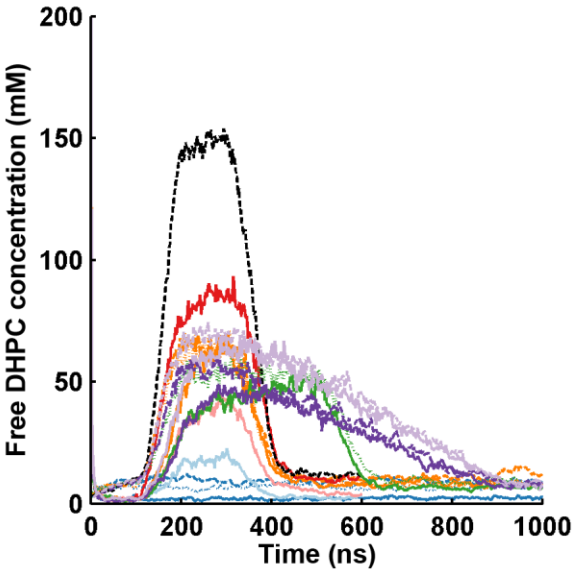

Figure S3. Free DHPC concentration plotted as function of time doing the different simulated annealing protocols. The descriptions of the lines are the same as in Figure S1.

After 900 ns the average aggregation number had almost converged to approximately 85 with the chosen protocol but the aggregation number distribution was rather broad (Figure S4). To evaluate if this was a result of the simulated annealing procedure, different SA protocols were tested. The large distribution might be due to the fast cooling period which could result in bicelles being trapped in metastable states. To test this hypothesis simulations were conducted where the cooling period was increased from 100 to 600 ns. The distribution obtained with this protocol was, however, very similar to the one obtained using the standard protocol with a wide size distribution with aggregation numbers up to approximately 200.

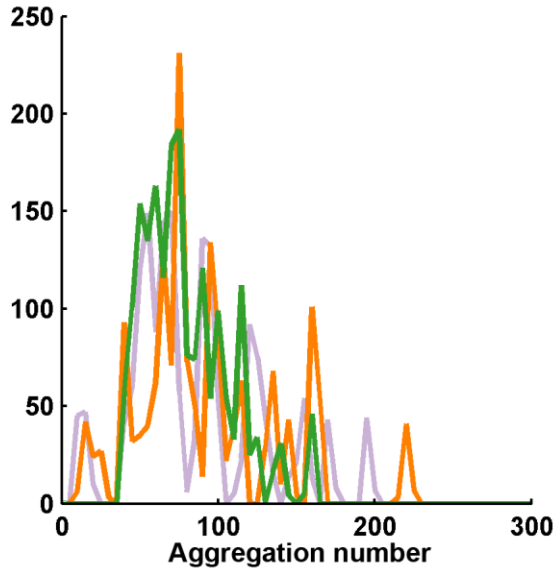

Figure S4. Aggregation number distribution observed in the 900-1000ns interval. The data is taken from 51 frames distributed evenly in the interval. The three lines are the standard protocol (orange), T_{max}=600 K and t_{max}=300ns (dark green), and T_{max}=700K and $t_{cooldown}$=600ns (light purple).

As seen from Figure S3 a large increase in free DHPC concentration was observed doing the increased temperature and some of the smaller aggregates in the distribution could be a consequence of this. Therefore, it would be of interest to reduce this. It is obvious from Figure S3 that the increase in free DHPC concentration was very dependent on the annealing temperature and on if only the lipids or the whole system was subject to the simulated annealing protocol. Since the free lipid concentration was significantly smaller when the system was increased to 600 K instead of 700 K, another protocol was tested where T_{max}= 600 K and t_{max}= 300 ns to see if an equilibrated system could be obtained with a lower increase in free DHPC concentration. This setup gave an average aggregation number just below 80 and some of the smallest and largest aggregates disappeared. The distribution in aggregation number was

however overall very similar with most of the aggregates positioned within the same interval as with the other two protocols. As all three protocols showed very similar distributions and the lower average aggregation number obtained with the decreased temperature protocol most likely was because equilibrium had not been reached, we went with the initial one as it was the most computational efficient protocol. To sum up, the systems were initially equilibrated for 100 ns at 308 K, heated to 700 K over another 100 ns, kept at 700 K for 100 ns, and cooled to 308 K over 100 ns. This procedure was followed by 600 ns of equilibration at 308 K and 1000 ns of production-run. The temperature of the solvent, lipids, and protein was controlled separately, and only the lipids were subject to the simulated annealing protocol.

Nanodiscs with a diameter of approximately 10 nm were constructed by combining the α-helical peptide MSP-Δ1-11, used by Shih et al. and available online,[6,7] with 150 DMPC lipids cut out of the bilayer simulation (75 lipids in each leaflet). The system was solvated, neutralized with sodium ions, and copied twice in each direction prior to simulation. This resulted in a total of eight nanodiscs placed 12.3 nm apart. As the secondary structure of proteins in the MARTINI force field is fixed, the MSP's was simulated as ten helix repeats as previously predicted and later found by NMR and X-ray crystalography[8,9] separated by dipeptide turn segments. The helix segments were residue 1-10, 13-32, 35-43, 46-65, 68-87, 90-109, 112-131, 134-153, 156-164, and 167-189. The simulation was named *Nanodisc*.

Membrane Mimics with KALP21. For the KALP21 simulations, four peptides were embedded into a pre-equilibrated DMPC bilayer in a transmembrane conformation with a random rotation along their helix axis. This gave a peptide:lipid ratio of 1:75 similar to the q=0.5 bicelle experiments conducted by Lind et al.[3] Equilibration of the peptides in the membrane without deletion of lipids was achieved by a minimization followed by a 40 ps simulation with 1 fs time

step and 1000 ns equilibration under standard conditions. This was followed by a 1000 ns production-run. The simulation will be referred to as *BilayerKALP*.

Small bicelles with KALP21 peptides bound were modelled by self-assembling the bicelles using the simulated annealing protocol described above for pure bicelles. The systems contained 3000 lipids and 40 KALP21 peptides each, which were randomly distributed in the simulation box likewise resulting in a peptide:lipid ratio of 1:75 (simulations named *Bicelle0q5KALP*). The large bicelle with KALP21 peptides bound was constructed by taking the bicelle obtained in the last frame of *Bicelle3q2* and placing 30 KALP21 peptides in the bicelle in a transmembrane orientation on a 6 by 5 grid with grid points spaced 3 nm apart. This gave a peptide:lipid ratio of approximately 1:75. Overlapping lipids were moved slightly away from the peptides to allow for insertion without deletion of lipids. The 34 free DHPC lipids that were removed during the isolation of the large bicelle were re-introduced randomly around the bicelle together with water and counter ions. This simulation was called *Bicelle3q2KALP*. In both the small and the large bicelle simulation, the systems were neutralized with chloride ions.

For simulations with KALP21 inserted into the nanodiscs, a disc of the same size as in the nanodiscs simulations without peptides was cut from a bilayer where the lipids had equilibrated for 100 ns around two fixed inserted peptides. The coarse grained MSP structure, water and counter ions were added, and the system was copied in all three dimensions, resulting in eight nanodiscs each consisting of 140 lipids, 2 KALP peptides, and 2 MSPs. The system was simulated under the name *NanodiscKALP*.

Modelling Membrane Mimics with Rhodopsin. Rhodopsin is known to form at least dimers[10,11] and a recent study combining MARTINI CG simulation and chemical crosslinking evaluated which dimer conformation seemed to be the most stable one.[10,12] The dimer simulated here was

initially oriented in its preferred conformation found in that study[12] and ELnedyn[13] was applied to maintain the structure of the individual rhodopsin monomers, requiring a reduction in the time step used; a 15 fs time step was thus applied in all simulations with rhodopsin.

The bilayer simulations with a rhodopsin dimer were built by initially placing the dimer in a box with dimensions 12 nm x 12 nm x 5 nm followed by randomly distributing 300 DMPC molecules in the box. Afterwards, the box dimensions was increased to 12 nm x 12 nm x 12 nm and water and counter ions were added. The system was equilibrated for 105 ns with the protein position restrained allowing for the lipids to form a bilayer around the proteins before the 2100 ns of simulation without position restraints. This simulation will be referred to as *BilayerRho*. The slight difference in simulation time compare to the simulations without rhodopsin was due to the difference in time step.

A rhodopsin dimer was embedded in the q=3.2 bicelle isolated from the last snapshot from the simulation of the large bicelle by deleting lipids within 5 Å of the proteins as well as 18 randomly chosen DHPC molecules to keep a q-value of 3.2. Water and counter ions were added and the system was simulated for 2100 ns in the simulation named *Bicelle3q2KALP*.

For simulations with rhodopsin inserted into the nanodiscs, the lipids and inserted proteins were cut out of a bilayer where the lipids had equilibrated for 105 ns around the fixed protein dimer. The radius of the circle cut out was the same as that used for the nanodisc without rhodopsin. This resulted in 8 nanodiscs consisting of 96 lipids, one rhodopsin dimer and two MSPs. The simulation will be referred to as *NanodiscRho*.

Analyses

Area per lipid for the DMPC bilayer was calculated by measuring the box dimensions in the plane of the bilayer and dividing it by the number of lipids in each leaflet. The thickness of the bilayer was measured from the z-distance between the average position of the glycerol beads in the upper and lower leaflet. The equivalent position in an atomistic setup was calculated from the center of mass of C2, C21, O21, and O22 and the center of mass of C3, C31, O21, and O22 for each lipid representing the GL1 and the GL2 beads, respectively. The atomistic simulation of a DMPC bilayer previously published[14] was used for comparison and the snapshots for the 25 to 100 ns time interval was used for this analysis.

The shape of the aggregates as well as the clustering of the individual molecules into aggregates was done as previously reported.[15] In short, the molecules were counted as part of the same aggregate if protein or lipid tail/glycerol linker beads were within 6 Å of each other. This distance includes the first interaction shell. The dimensions of the aggregates were found by measuring the maximum distance between beads within an aggregate along the three principal axes of inertia of the aggregate. In simulations including KALP21 or rhodopsin, these proteins were included in the evaluation of the inertia axes but ignored in the calculation of the membrane mimic dimensions to measure the true thickness of the membrane mimic. KALP21 oligomerization was characterized by defining the peptides to be in a cluster if any beads of the two peptides were closer than 6 Å.

To evaluate if the bicelles are described best by a mixed micelle model, where the two lipids are completely mixed, or by a model where the lipids are segregated in two domains, the average fraction of DMPC neighbors was measured for each individual lipid molecule, and the DMPC cluster sizes were computed. If the lipids were totally mixed the fraction of DMPC neighbors for

DHPC and DMPC should be the same and close to the DMPC:DHPC ratio participating in bicelles. However, if domains were formed, DMPC would show an increased fraction of DMPC neighbors, while DHPC would show a decreased fraction of DMPC neighbors. To evaluate this, Voronoi tessellation was employed with the program Voro++ 0.4.5.[16] In Voronoi calculations, the space of the simulation box is assigned to a given bead according to which bead it is closest to. The result is that smaller polygonal boxes centered on each bead are formed, where all points on the polygons facets are defined by being equally close to the two beads that facet separates. Each aggregate was isolated before the Voronoi calculation. In this analysis two lipid were defined as being neighbors if one of the lipid's glycerol linker beads shared a facet with the other lipid's glycerol linker beads. This choice was made to avoid lipids on opposite sides of the bicelle to be assigned neighbors. The analysis slightly underestimates the DHPC contacts compared to DMPC contacts due to the higher dynamics and curvature of DHPC, which results in DHPC not being as well aligned in the surface of the aggregates; however we do not expect this to affect the overall conclusions. The neighbors of the KALP21 peptides were found by measuring the contacts between any KALP21 bead and the lipids' glycerol linker beads. The same technique was used to count the number lipids with the glycerol linker in contact with the different beads in KALP21 defining which part of the peptide was in contact with the hydrophilic part of the lipids. To compare the interaction of KALP21 in different environment the values of each lipid type in each environment was normalized so the maximum interaction equaled one.

The solvent accessible surface area (SASA) was measured by use of Voronoi tessellation as described above; however, the calculations were done on the full system, where only the charged interaction sites of the water beads were removed, since they have no van der Waals interactions.

The SASA of a molecule was defined as the total surface area shared between the water beads and any of the beads in that molecule.

The tilt angle of the KALP21 with respect to the membrane normal was calculated in all membrane mimics except the bilayers by aligning the aggregates with the principal axis of inertia with the highest principal value along the z-axis and measuring the angle between the z-axis and the vector defined as going from the center of mass (COM) of the backbone bead of residue 1-4 to the COM of the backbone beads of residue 18-21. In the bilayers the bilayer normal was assumed to be aligned the z-axis, and the angles were measured with respect to this axis.

The contact time between a lipid and the rhodopsin molecules was calculated by measuring when approximately 40 % of the lipid's beads (2 for DHPC and 4 for DMPC) were within 7 Å of the protein. If the contact was lost or present for less than 12 ns (6 sequential snapshots) the change was ignored. When evaluating the contact time to the individual helices only 1 lipid bead had to be within the cutoff of the helix for the contact to be present.

Calculation of NMR Spectra for Large Bicelles. Large bicelles ($q \gtrsim 2$) in aqueous solution orient in a strong magnetic field with the bicelle normal perpendicular to the direction of the magnetic field.[17] Since the force fields used in the present MD simulations do not include the magnetic susceptibility effects governing the alignment, we have aligned the bicelles in each snapshot before calculating the nuclear interaction parameters for the lipids as described elsewhere.[14] In brief, the alignment is such that the largest principal element of their inertia moment tensor is aligned along the z axis of an alignment frame.

In the alignment frame we may calculate the orientation of the ^{31}P chemical shift tensor assuming a particular orientation of the tensor in the coordinate system defined by the PO4, GL1, and GL2 beads, derived from a detailed comparison of AA and CG bilayer systems.[14] The final

transformation to the laboratory frame involves a scaling of the orientation-dependent ^{31}P chemical shift by a second-order Legendre polynomial $(3\cos^2 90° - 1)/2 = -1/2$, which arises from the perpendicular orientation of aligned bicelles with respect to the magnetic field. The simulated ^{31}P NMR spectra are obtained by adding peaks corresponding to the time- and ensemble averaged frequencies for the ^{31}P chemical shifts in DMPC and DHPC. Likewise, the order parameters of the bonds in the CG description of DMPC were calculated from the aligned bicelle with the formula $P_2 = 0.5\langle 3\cos^2\theta - 1\rangle$ where θ is the angle between the bond and the bicelle normal.

Figures

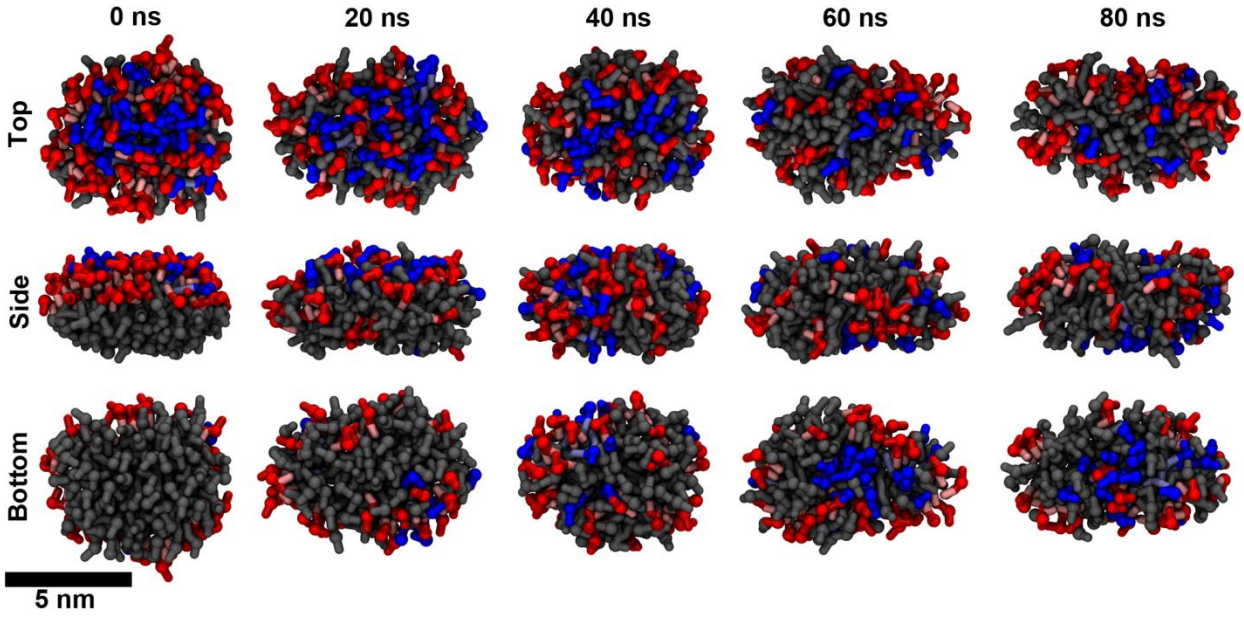

Figure S5. Pictures of the diffusion of lipids within a q=0.5 bicelle which changed its shape. The aggregation number is approximately 135 (somewhat larger than the average of 91). Consecutive pictures from left to right show the time development of a bicelle spaced 20 ns apart and viewed from three different orientations: Top, side, and bottom. Lipids with their phosphate bead

initially below the center of the bicelle with respect to the short dimension are colored gray while lipid with their phosphate bead initially above the center are colored according to the lipid type; red for DHPC and blue for DMPC. The lipids are observed to quickly mix and furthermore, it is seen that the bicelle changed from an oblate to a prolate shape within 80 ns of simulation.

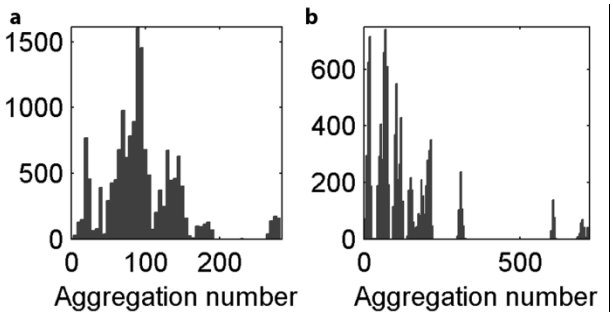

Figure S6. The observed distribution in aggregation number for q=0.5 bicelle doing the last μs of simulation. Systems started from a) disc with a radius of 3 nm (*Bicelle0q5r3*) and b) disc with radius of 5 nm (*Bicelle0q5r5*).

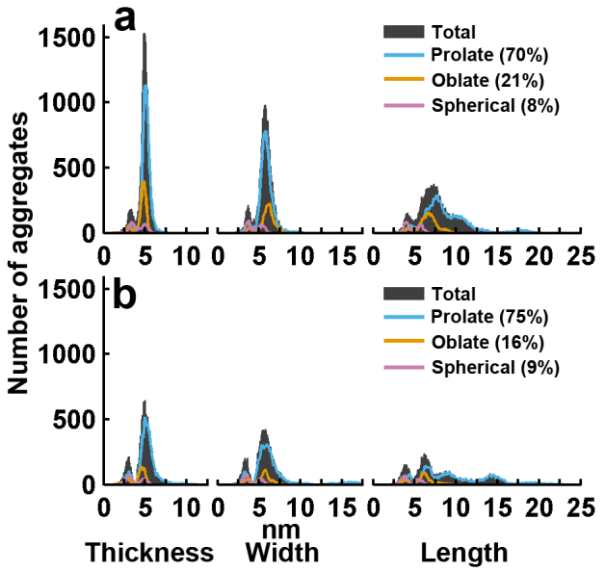

Figure S7. Size and shape of the aggregates observed in simulations started form discs with a radius of a) 3nm (*Bicelle0q5r3*) and b) 5 nm (*Bicelle0q5r5*).

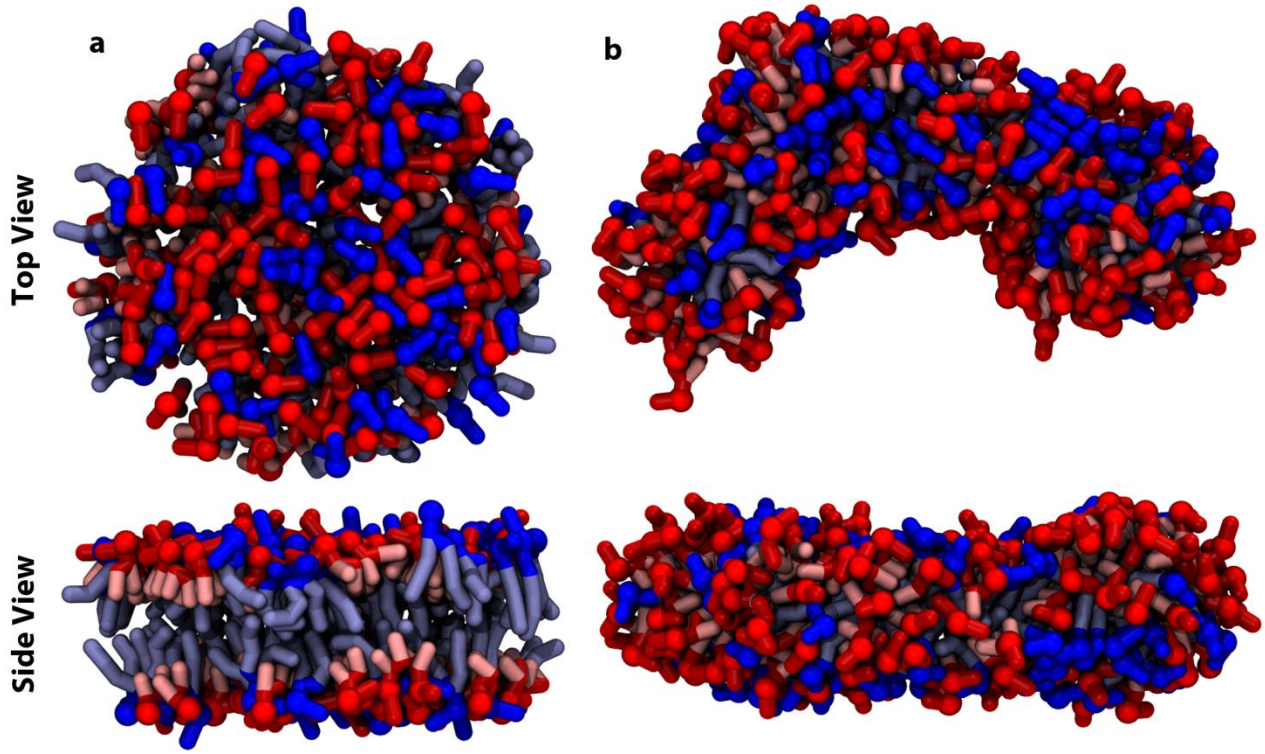

Figure S8. A q=0.5 bicelle build as a disc with a radius of 5 nm shown from the top and from the side a) prior to MD simulation and b) after 100 ns of MD simulation.

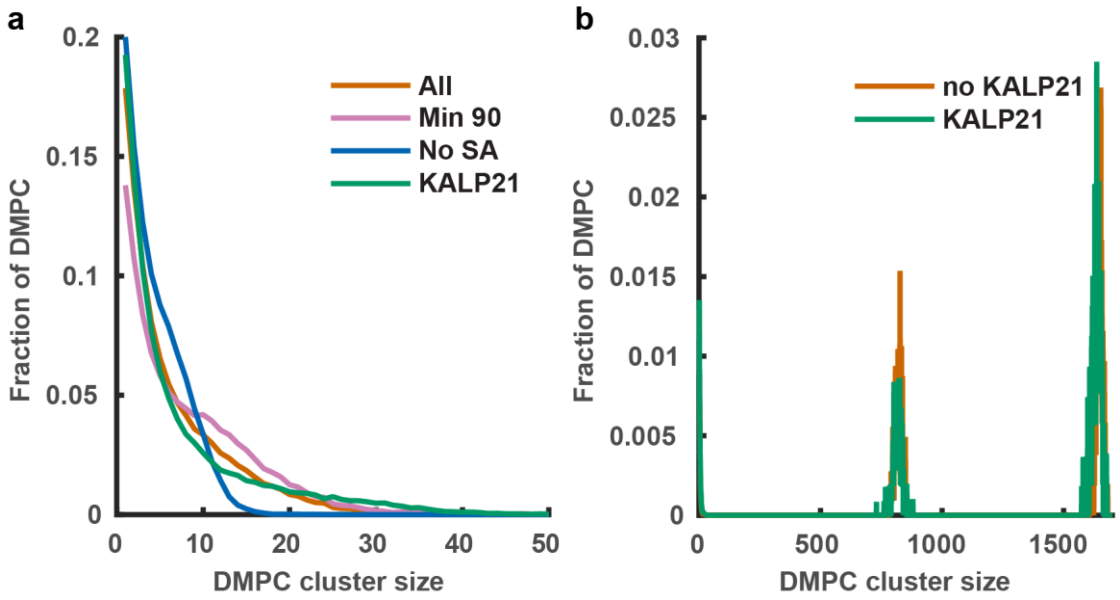

Figure S9. Fraction of the DMPC molecules in a cluster of a given size for a) q=0.5 bicelles and b) q=3.2 bicelles.

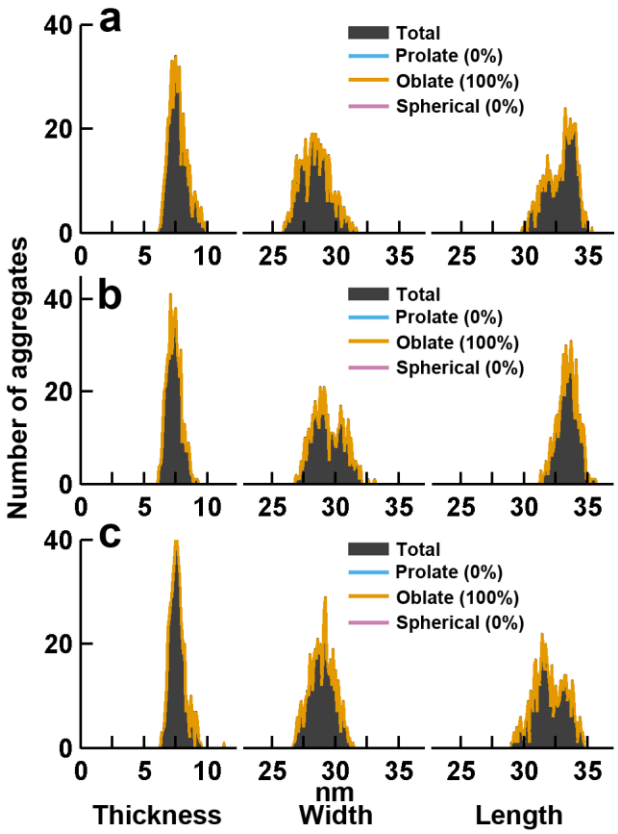

Figure S10. Distribution of the shape and size of a) the large bicelle (*Bicelle3q2*), b) the large bicelle with KALP21 peptides (*Bicelle3q2KALP*), and c) the large bicelle with a rhodopsin dimer embedded (*Bicelle3q2Rho*).

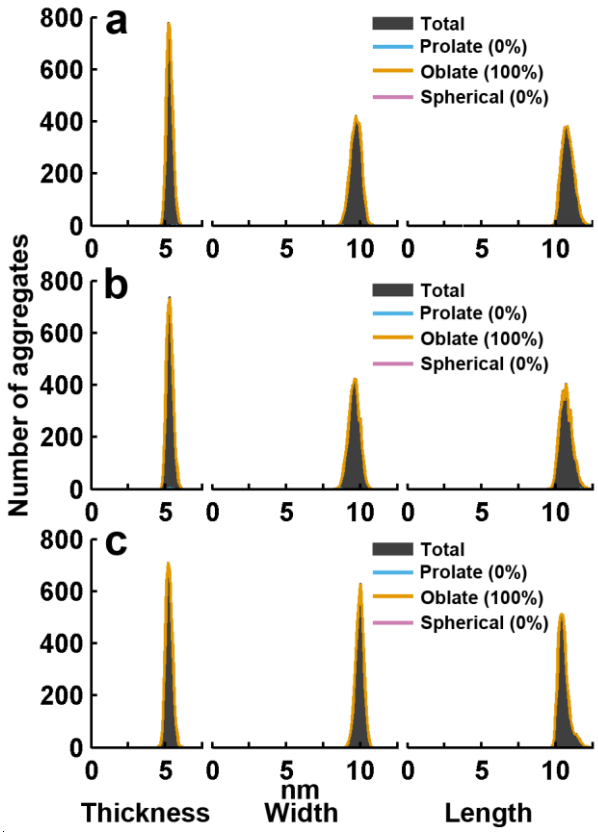

Figure S11. Distribution of the nanodiscs dimensions and shape in a) nanodiscs (*Nanodisc*), b) nanodiscs with KALP21 (*NanodiscKALP*), and c) nanodiscs with rhodopsin (*NanodiscRho*).

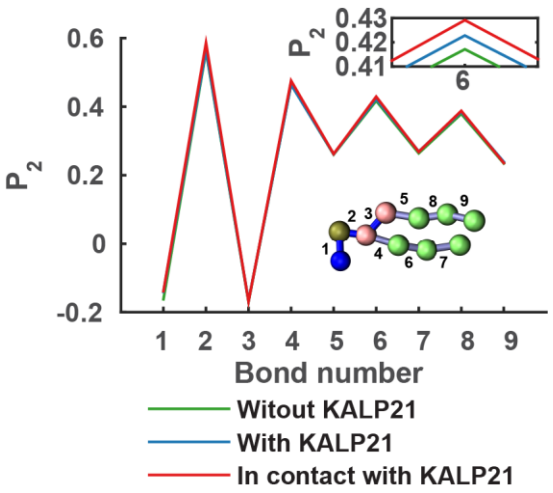

Figure S12. Order parameter, P_2, for each CG bond in DMPC. Top insert show a zoom-in of the sixth bond to illustrate the typical difference in order parameter observed. Bottom insert show the DMPC lipid with bond numbers defined. Green line describe all DMPC in *Bicelle3q2* while blue and red line represent all DMPC lipids or only the DMPC lipids in contact with KALP21, respectively, in *Bicelle3q2KALP*.

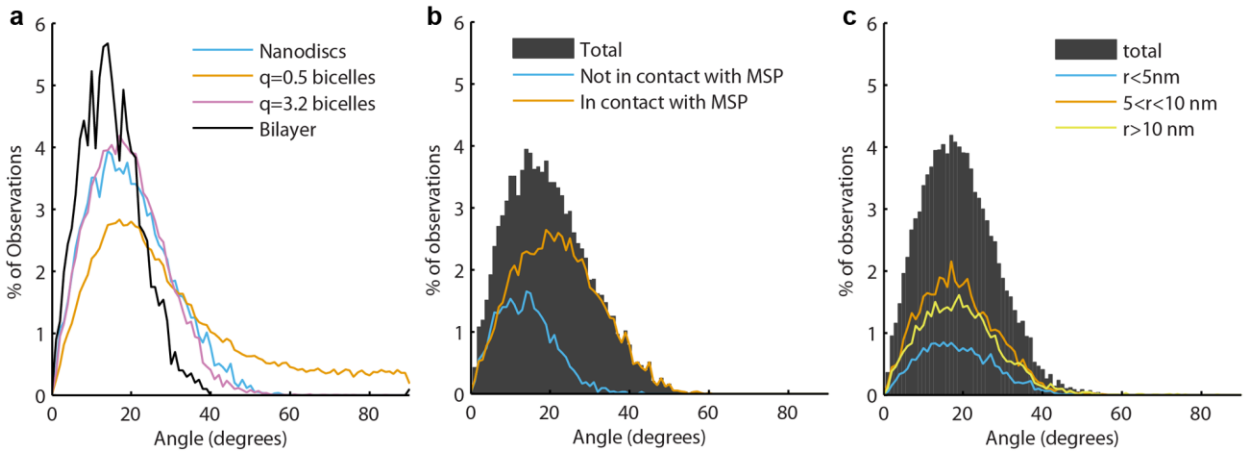

Figure S13. The tilt angle distribution of KALP21 in different membrane mimics. a) Comparison of the angle distribution in different membrane mimics; b) the angle distribution in nanodiscs where the peptides have been divided according to if they are in contact with the

MSPs or not; and c) the distribution in tilt angle of KAL21 in q=3.2 bicelles in different intervals of the distance to the bicelle center.

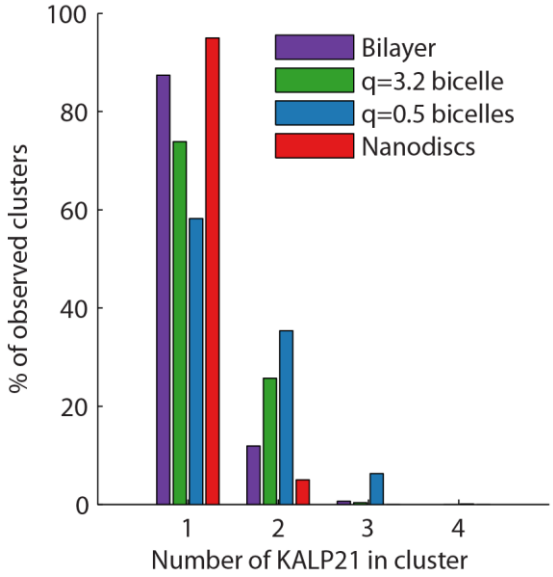

Figure S14. Oligomerization of the KALP21 peptide in the different membrane mimics.

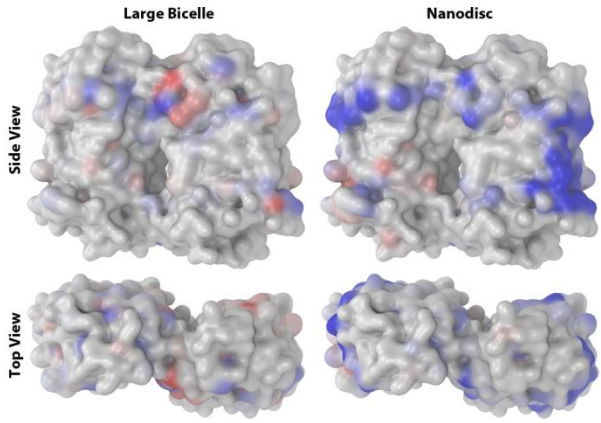

Figure S15. Solvation of rhodopsin in a large bicelle and in a nanodisc compared to in a bilayer. Blue color indicates areas that are more solvated in the mimic than in a bilayer while red indicate areas that are less solvated than in a bilayer.

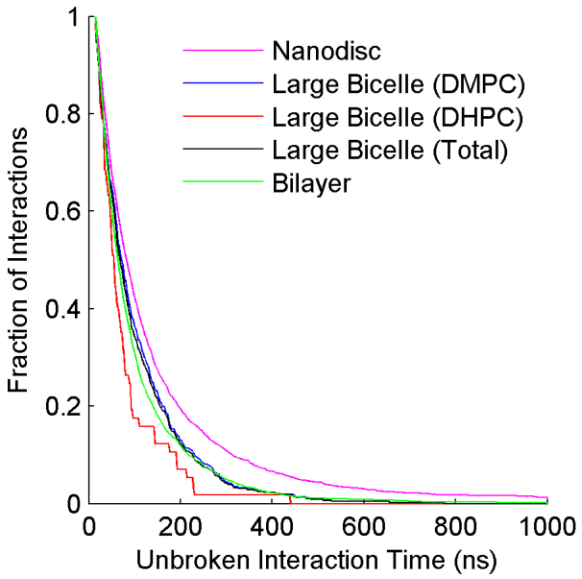

Figure S16. The fraction of the observed interactions that last for at least a given time interval as function of the time interval.

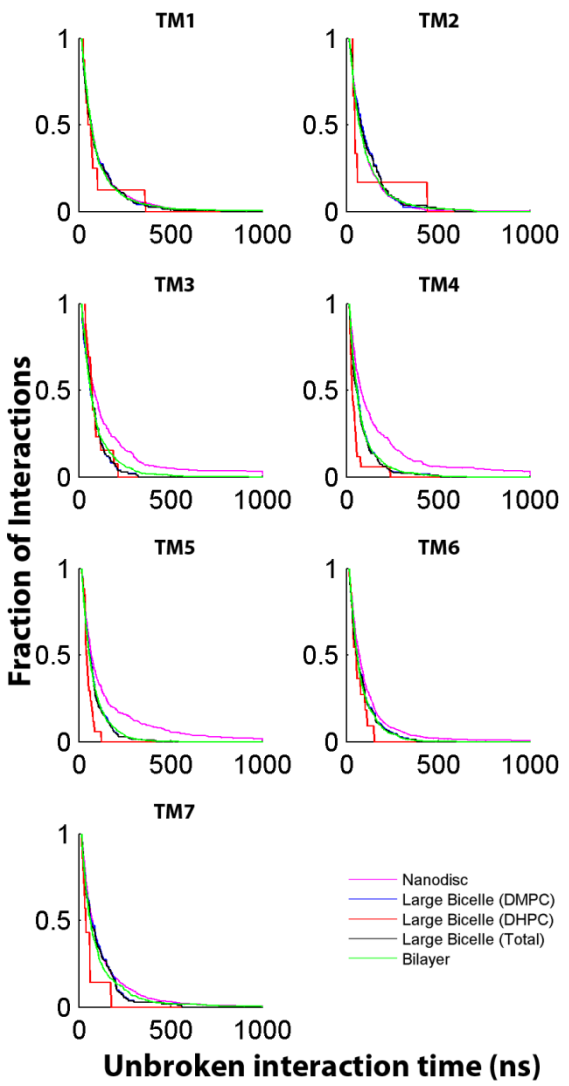

Figure S17. The fraction of the observed interactions for each individual transmembrane helix (TM) in rhodopsin that last for at least a given time interval as function of the time interval.

References

(1) Humphrey, W.; Dalke, A.; Schulten, K. VMD: Visual Molecular Dynamics. *J. Mol. Graphics* **1996**, *14*, 33-38.

(2) van Dam, L.; Karlsson, G.; Edwards, K. Direct Observation and Characterization of DMPC/DHPC Aggregates Under Conditions Relevant for Biological Solution NMR. *Biochim. Biophys. Acta, Biomembr.* **2004**, *1664*, 241-256.

(3) Lind, J.; Nordin, J.; Mäler, L. Lipid Dynamics in Fast-Tumbling Bicelles with Varying Bilayer Thickness: Effect of Model Transmembrane Peptides. *Biochim. Biophys. Acta, Biomembr.* **2008**, *1778*, 2526-2534.

(4) Glover, K. J.; Whiles, J. A.; Wu, G.; Yu, N.; Deems, R.; Struppe, J. O.; Stark, R. E.; Komives, E. A.; Vold, R. R. Structural Evaluation of Phospholipid Bicelles for Solution-State Studies of Membrane-Associated Biomolecules. *Biophys. J.* **2001**, *81*, 2163-2171.

(5) Ye, W.; Lind, J.; Eriksson, J.; Mäler, L. Characterization of the Morphology of Fast-Tumbling Bicelles with Varying Composition. *Langmuir* **2014**, *30*, 5488-5496.

(6) Shih, A. Y.; Denisov, I. G.; Phillips, J. C.; Sligar, S. G.; Schulten, K. Molecular Dynamics Simulations of Discoidal Bilayers Assembled from Truncated Human Lipoproteins. *Biophys. J.* **2005**, *88*, 548-556.

(7) *http://www.ks.uiuc.edu/* (accessed August 31th, 2014).

(8) Nolte, R. T.; Atkinson, D. Conformational Analysis of Apolipoprotein A-I and E-3 Based on Primary Sequence and Circular Dichroism. *Biophys. J.* **1992**, *63*, 1221-1239.

(9) Cushley, R. J.; Okon, M. NMR Studies of Lipoprotein Structure. *Annu. Rev. Biophys. Biomol. Struct.* **2002**, *31*, 177-206.

(10) Knepp, A. M.; Periole, X.; Marrink, S.; Sakmar, T. P.; Huber, T. Rhodopsin Forms a Dimer with Cytoplasmic Helix 8 Contacts in Native Membranes. *Biochemistry* **2012**, *51*, 1819-1821.

(11) Fotiadis, D.; Liang, Y.; Filipek, S.; Saperstein, D. A.; Engel, A.; Palczewski, K. The G Protein-Coupled Receptor Rhodopsin in the Native Membrane. *FEBS Lett.* **2004**, *564*, 281-288.

(12) Periole, X.; Knepp, A. M.; Sakmar, T. P.; Marrink, S. J.; Huber, T. Structural Determinants of the Supramolecular Organization of G Protein-Coupled Receptors in Bilayers. *J. Am. Chem. Soc.* **2012**, *134*, 10959-10965.

(13) Periole, X.; Cavalli, M.; Marrink, S. J.; Ceruso, M. A. Combining an Elastic Network with a Coarse-Grained Molecular Force Field: Structure, Dynamics, and Intermolecular Recognition. *J. Chem. Theory Comput.* **2009**, *5*, 2531-2543.

(14) Hansen, S. K.; Vestergaard, M.; Thøgersen, L.; Schiøtt, B.; Nielsen, N. C.; Vosegaard, T. Lipid Dynamics Studied by Calculation of ^{31}P Solid-State NMR Spectra using Ensembles from Molecular Dynamics Simulations. *J. Phys. Chem. B* **2014**, *118*, 5119-5129.

(15) Kraft, J. F.; Vestergaard, M.; Schiøtt, B.; Thøgersen, L. Modeling the Self-Assembly and Stability of DHPC Micelles using Atomic Resolution and Coarse Grained MD Simulations. *J. Chem. Theory Comput.* **2012**, *8*, 1556-1569.

(16) Rycroft, C. H. VORO++: A Three-Dimensional Voronoi Cell Library in C++. *Chaos* **2009**, *19*, 041111.

(17) Sanders, C. R.; Schwonek, J. P. Characterization of Magnetically Orientable Bilayers in Mixtures of Dihexanoylphosphatidylcholine and Dimyristoylphosphatidylcholine by Solid-State NMR. *Biochemistry* **1992**, *31*, 8898-8905.